

A Mathematical Framework for Understanding Four-Dimensional Heterogeneous Differentiation of CD4⁺ T Cells

Tian Hong · Cihan Oguz · John J. Tyson

Received: 14 April 2014 / Accepted: 2 March 2015 / Published online: 17 March 2015
© Society for Mathematical Biology 2015

Abstract At least four distinct lineages of CD4⁺ T cells play diverse roles in the immune system. Both in vivo and in vitro, naïve CD4⁺ T cells often differentiate into a variety of cellular phenotypes. Previously, we developed a mathematical framework to study heterogeneous differentiation of two lineages governed by a mutual-inhibition motif. To understand heterogeneous differentiation of CD4⁺ T cells involving more than two lineages, we present here a mathematical framework for the analysis of multiple stable steady states in dynamical systems with multiple state variables interacting through multiple mutual-inhibition loops. A mathematical model for CD4⁺ T cells based on this framework can reproduce known properties of heterogeneous differentiation involving multiple lineages of this cell differentiation system, such as heterogeneous differentiation of T_H1–T_H2, T_H1–T_H17 and iT_{Reg}–T_H17 under single or mixed types of differentiation stimuli. The model shows that high concentrations of differentiation stimuli favor the formation of phenotypes with co-expression of lineage-specific master regulators.

Keywords CD4⁺ T cells · Cell differentiation · Mathematical model

1 Introduction

Immune responses are often complex in terms of the types of cells involved and the biochemical activities elicited in pathogenic events. To achieve accurate regulation of

Electronic supplementary material The online version of this article (doi:[10.1007/s11538-015-0076-6](https://doi.org/10.1007/s11538-015-0076-6)) contains supplementary material, which is available to authorized users.

T. Hong · C. Oguz · J. J. Tyson (✉)
Department of Biological Sciences, Virginia Polytechnic Institute and State University, Blacksburg,
VA 24061, USA
e-mail: tyson@vt.edu

various types of responses, the immune system has evolved delicate control mechanisms, including the differentiation of various subsets of CD4⁺ T cells (Luckheeram et al. 2012), which play diverse and important regulatory roles in immune responses. The best known subsets of CD4⁺ T cells are T helper 1 (T_H1), T helper 2 (T_H2), T helper 17 (T_H17) and induced regulatory T (iT_{Reg}) cells (Zhu et al. 2010). Each subset has a unique key transcription factor, known as a master regulator, which controls the lineage specification. The master regulators for the four subsets are T-bet, GATA3, ROR γ t and Foxp3, respectively (Fontenot et al. 2003; Ivanov et al. 2006; Szabo et al. 2000; Zheng and Flavell 1997). The progenitor cells of all four types of CD4⁺ cells are known as naïve CD4⁺ T cells. Once these cells are activated by antigen presentation and cytokines, they differentiate into functional CD4⁺ T cells. The key event of differentiation is the up-regulation of at least one master regulator (O’Shea and Paul 2010). The identities and strengths of the environmental cues, i.e., the exogenous signals, determine the lineage of the differentiated cell. For example, interleukin 12 (IL-12) induces naïve T cells to differentiate into T_H1 cells in the presence of antigenic agents that activate their T cell receptors (TCRs) (Hsieh et al. 1993).

It is not surprising that most immune responses elicit balanced phenotypes of CD4⁺ T cells (Murphy and Stockinger 2010; O’Shea and Paul 2010). Interestingly, even under uniform exposure of a single pool of naïve CD4⁺ T cells to a specific combination of exogenous signals, multiple lineages of differentiated T cells may arise. Such ‘induced’ heterogeneous differentiation suggests that balanced immune responses observed *in vivo* may not be due solely to heterogeneous microenvironments of the cells. Rather, specific regulatory mechanisms may be responsible for heterogeneous types of differentiation.

Previously, we developed a mathematical framework for analyzing heterogeneous differentiation involving two master regulators (Hong et al. 2011, 2012). However, cross talk among all four master regulators is important for the specification of CD4⁺ T cell lineages. Some recent mathematical models for CD4⁺ T cells have included signaling networks with more than two master regulators, and they can be used to explain the differentiation of naïve CD4⁺ T cells into each of the four lineages (Mendoza 2013; Naldi et al. 2010). However, these models do not explain how naïve CD4⁺ T cells can differentiate heterogeneously into combinations of the four lineages. Moreover, the lack of analytic tools for multi-stability behaviors governed by complex mutual-inhibition relationships has limited our understanding of this differentiation system. Here, we present a framework that can be used to study multi-stability behavior involving networks with multiple interconnected mutual-inhibition motifs involving three or four master regulators. We use this framework to build a model of CD4⁺ T cell differentiation with four master regulators and to explain the heterogeneous differentiations that involve these regulators.

2 Results

2.1 A Threefold Symmetrical Differentiation System

Building on our previous studies of the interactions of two master regulators (Hong et al. 2011, 2012), we first analyzed a signaling network motif with three master

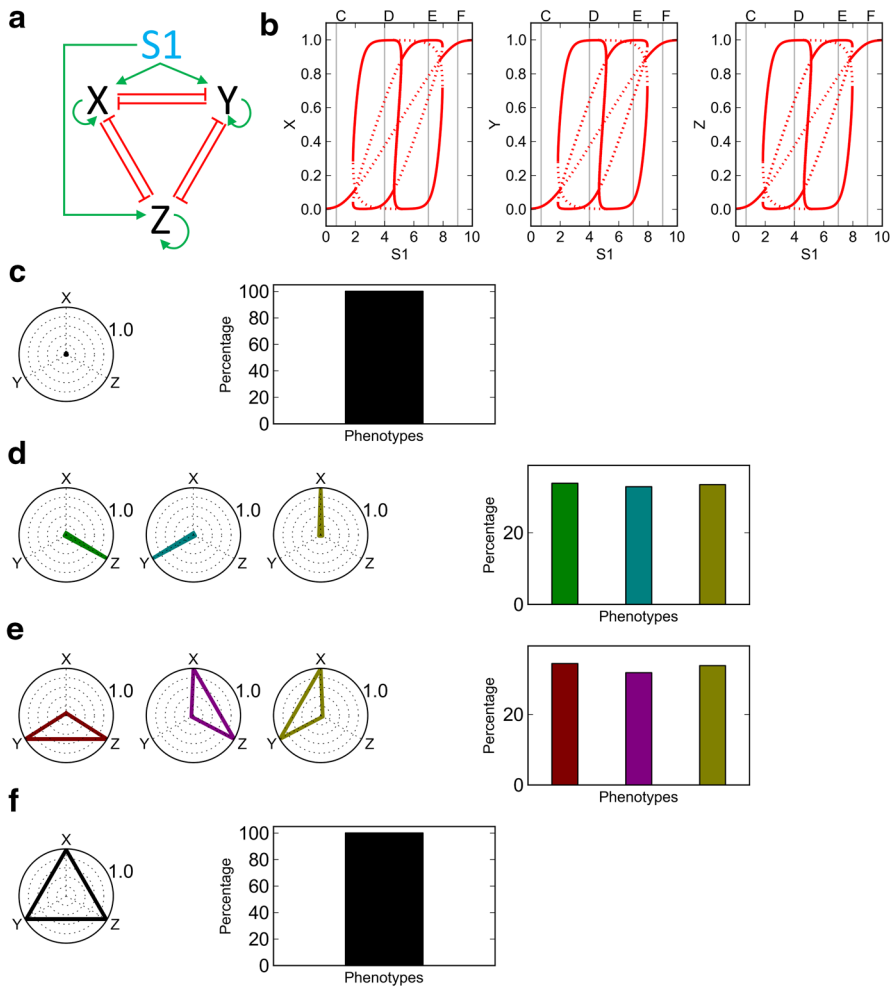


Fig. 1 Analysis of a motif with three master regulators. **a** Influence diagram of the model. **b** Bifurcation diagrams with respect to $S1$. *Solid curves* stable steady states. *Dashed curves*: unstable steady states. *Vertical gray lines*: references to stability analysis with specific control parameter values shown in following sub-figures. **c-f** Radar plots: representation of stable steady states. In each radar plot, expression levels of master regulators are plotted on the axes. Bar charts: the phenotypic composition of a simulated cell population at $t_{end} = 7$ (Color figure online)

regulators, X, Y and Z. Each pair of master regulators interacts by mutual inhibition, and each master regulator activates its own production. A differentiation signal $S1$, which represents the antigenic stimulus, activates the production of all three master regulators (Fig. 1a). We start with a set of basal parameter values (Supplementary Table S1) that correspond to symmetrical interactions among all three components.

The bifurcation diagram (Fig. 1b) for the differentiation signal $S1$ reveals that the system has one stable steady state for $0 \leq S1 < 1.8$ (e.g., Fig. 1b vertical line C). This state corresponds to the naïve cell, since all three master regulators are expressed

at low levels (Fig. 1c, radar plots). When a population of cells was simulated with the indicated amount of signal S1, all cells in the population were still in the naïve state at the end of the simulation (Fig. 1c, bar chart).

At $S1 \approx 2$, there occurs a subcritical pitchfork bifurcation with threefold symmetry: The system changes from one naïve state (Fig. 1c) to three single-positive stable steady states (Fig. 1d) and four other unstable steady states (not shown; we focus on analyzing stable steady states in this study). In the range $1.8 < S1 < 4.5$, the system is tri-stable, and the simulated cell population became heterogeneous, containing comparable fractions of three single-positive phenotypes at the end of the simulation (Fig. 1d, bar chart).

At $S1 \approx 5$, two further pitchfork bifurcations occur. Each single-positive state changes to two stable steady states via a supercritical pitchfork bifurcation with twofold symmetry, forming six stable steady states in total, and at a slightly higher signal strength ($S1 \approx 5.5$), the system undergoes additional pitchfork bifurcations which change these six stable steady states back to three stable steady states. These three new stable steady states correspond to double-positive phenotypes (Fig. 1e). In the range $5.5 < S1 < 7.5$, the system is tri-stable, and the simulated cell population became heterogeneous, containing comparable fractions of three double-positive phenotypes at the end of the simulation (Fig. 1e, bar chart).

At $S1 \approx 7.5$, the system undergoes another subcritical pitchfork bifurcation with threefold symmetry, changing the three double-positive stable steady states to one triple-positive steady state, and the system is mono-stable for $S1 > 7.5$ (Fig. 1f).

A more abstract approach was used by [Ball and Schaeffer \(1983\)](#) and [Golubitsky et al. \(1988\)](#) to analyze similar types of symmetrical bifurcations. More detailed discussion of the bifurcation diagram in Fig. 1b is presented in the Supplementary Text.

2.2 An Asymmetrical Differentiation System

We next analyzed a system with broken symmetry to illustrate how an asymmetrical model differs from a symmetrical one. An asymmetrical model can be obtained by making small perturbations to the model described in the previous subsection. In particular, we changed the basal activation-state parameter for X from $\omega_X^0 = -2$ to -2.1 and that for Y from $\omega_Y^0 = -2$ to -1.9 . Random perturbations of all parameter values give similar results (not shown). Typically, the steady states of an asymmetrical system have profiles similar to the bifurcation diagram shown in Fig. 2a.

Briefly, the asymmetrical model breaks the symmetry of the pitchfork bifurcations in the symmetrical model. Similar to the symmetrical model, with increasing S1 the system bifurcates from a mono-stable naïve state (Fig. 2a vertical lines B and Fig. 2b) to a system with three stable steady states (Fig. 2a vertical lines C and Fig. 2c), but only one of these differentiated states is connected to the naïve state. The other two curves, corresponding to single-positive states, form two loops ('isolas'), disconnected from the main branch of solutions. Each isola is bounded by two saddle-node bifurcation points (for best illustration, see left plot of Fig. 2a vertical line C). In terms of cell differentiation, one of the three single-positive phenotypes is favored because of the broken symmetry and is more abundant in the final state of the simulation (Fig. 2c, bar chart).

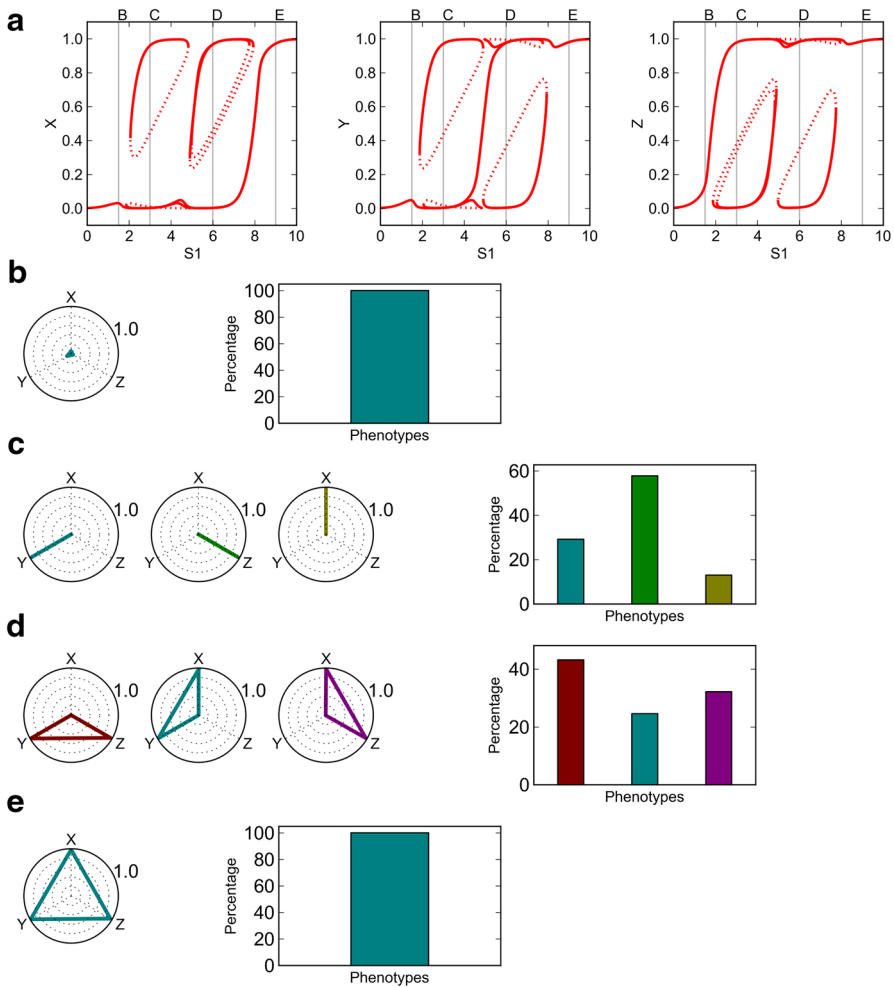


Fig. 2 Analysis of a motif with three master regulators with broken symmetry. **a** Bifurcation diagrams with respect to S_1 . *Solid curves, dashed curves and vertical gray lines* as in Fig. 1. **b–e** Radar plots and bar charts as in Fig. 1 (Color figure online)

For larger values of S_1 , three double-positive states exist in the system (Fig. 2a vertical lines D and Fig. 2d), and for larger values still, the system has a single triple-positive steady state (Fig. 2a vertical lines E and Fig. 2e).

2.3 A Fourfold Symmetrical Differentiation System

Using the same strategy, we analyzed a system with four master regulators W , X , Y and Z (Fig. 3a). The parameter values listed in Supplementary Table S2 refer to a symmetrical system.

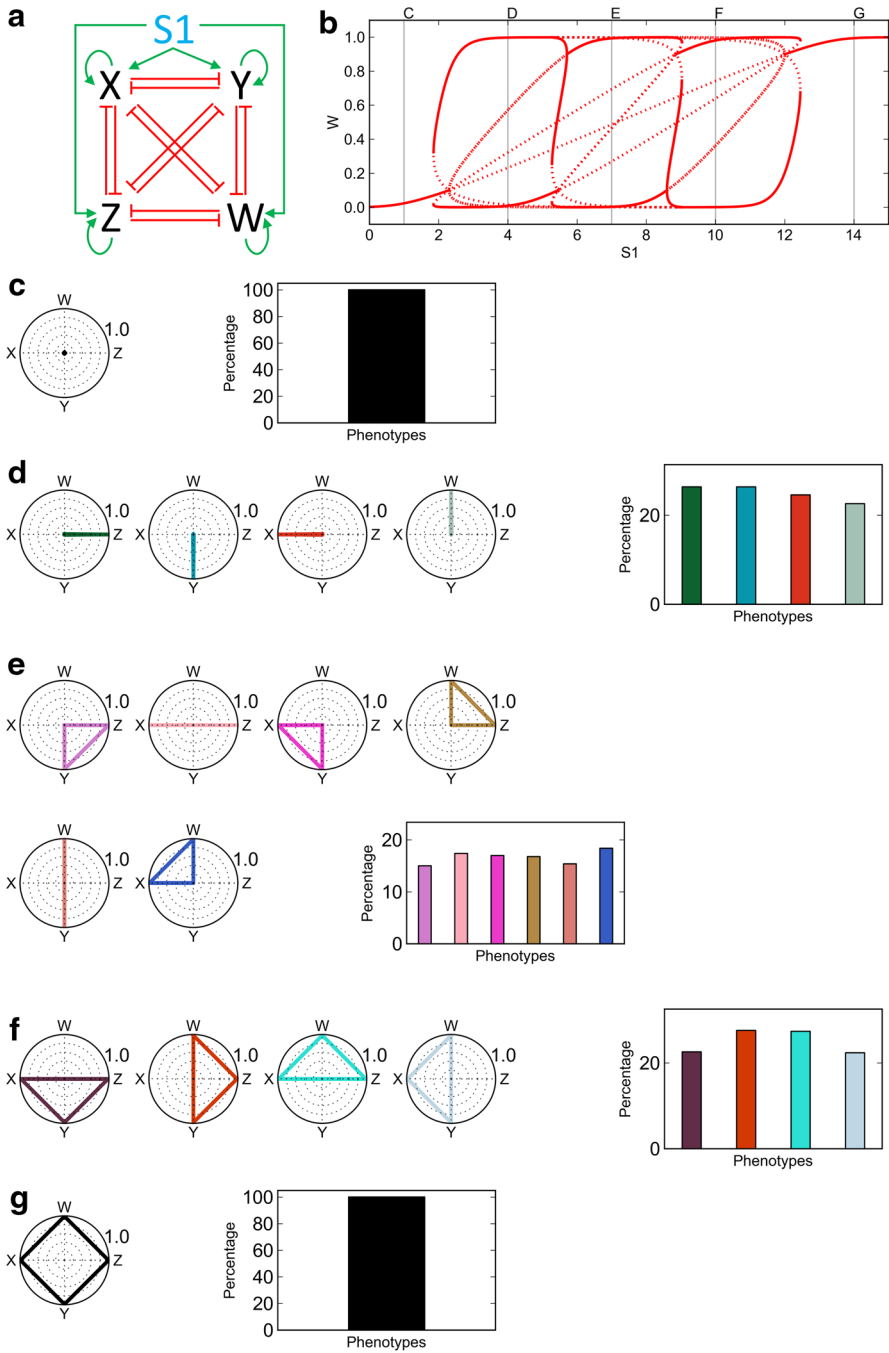


Fig. 3 Analysis of a motif with four master regulators. **a** Influence diagram of the model. **b** Bifurcation diagram with respect to S1. *Solid curves, dashed curves and vertical gray lines* as in Fig. 1. **c–g** Radar plots and bar charts as in Fig. 1 (Color figure online)

We plot the bifurcation diagram for state variable W in Fig. 3b; the diagrams for the other three state variables are similar. The system is mono-stable with one naïve state for $0 \leq S1 < 1.8$ (Fig. 3b vertical line C and Fig. 3c). At $S1 \approx 2$, the system undergoes subcritical bifurcations with fourfold symmetry, and the system is tetra-stable (four single-positive, stable steady states) in the range $2.5 < S1 < 5.3$ (Fig. 3b vertical line D and Fig. 3d). At $S1 \approx 5.5$, the system undergoes a pair of pitchfork bifurcations, one with threefold symmetry and the other with twofold symmetry, changing the four stable steady states to six double-positive steady states (Fig. 3b vertical line E and Fig. 3e). At $S1 \approx 9$, the system undergoes another pair of pitchfork bifurcations, changing the six stable steady states to four triple-positive steady states (Fig. 3b vertical line F and Fig. 3f). At $S1 \approx 12$, the system undergoes a pitchfork bifurcation with fourfold symmetry and becomes mono-stable for $S1 > 12$ (Fig. 3b vertical line G and Fig. 3g). Due to the symmetrical nature of the system, in each of these multi-stable regions, comparable fractions of the phenotypes were obtained in the simulation (bar charts in Fig. 3d–f).

As an example for an asymmetrical model with four master regulators, we present a model for $CD4^+$ T cell differentiation in the next subsection.

2.4 A System for $CD4^+$ T Cell Differentiation with Four Master Regulators

Our model for $CD4^+$ T cell differentiation is diagrammed in Fig. 4a. In addition to the TCR signal, which is an example of the $S1$ signal previously analyzed, we introduced various cytokines to the model. These cytokines serve as ‘polarizing’ signals that can bias the differentiation into one (e.g., IL-4) or more (e.g., TGF- β) phenotypes. Parameter values for this model are listed in Supplementary Table S3. These values were optimized to give a good fit to the experimental observations listed in Table 1. Basically, we simulated the experimental conditions in Table 1 by inducing cell differentiation in our model equations with various exogenous signals and recording the derived cell populations. Then, we varied the parameter values of the model (ranges given in Supplementary Table S3) to optimize the fit of the model’s predictions to the observed cell populations (Table 1). The optimization algorithm is described in the Methods section. After optimizing our model in this way, we used our mathematical framework to analyze some of the key facts regarding heterogeneous differentiation.

With the T cell receptor signal alone, the model system can be multi-stable, exhibiting all four single-positive states and the T-bet-ROR γ t double-positive state (Fig. 4b, vertical lines C and Fig. 4c). When a population of simulated cells was exposed to the TCR signal alone (Fig. 4c, bar chart), eighty percent of the population became positive for T-bet (i.e., T_H1 cells), and twenty percent expressed GATA3 (i.e., T_H2 cells). When the population was treated with higher strengths of TCR signal, a higher fraction of T_H2 cells was obtained (Fig. 4d, e), in agreement with experimental results by Yamashita et al. (1999). Interestingly, the model suggests that, although other single-positive states are stable under TCR-activated conditions (without any other exogenous signals), these phenotypes cannot be obtained by treating with TCR signal alone. In the presence of both T_H1 and T_H2 promoting cytokines, TCR induced the

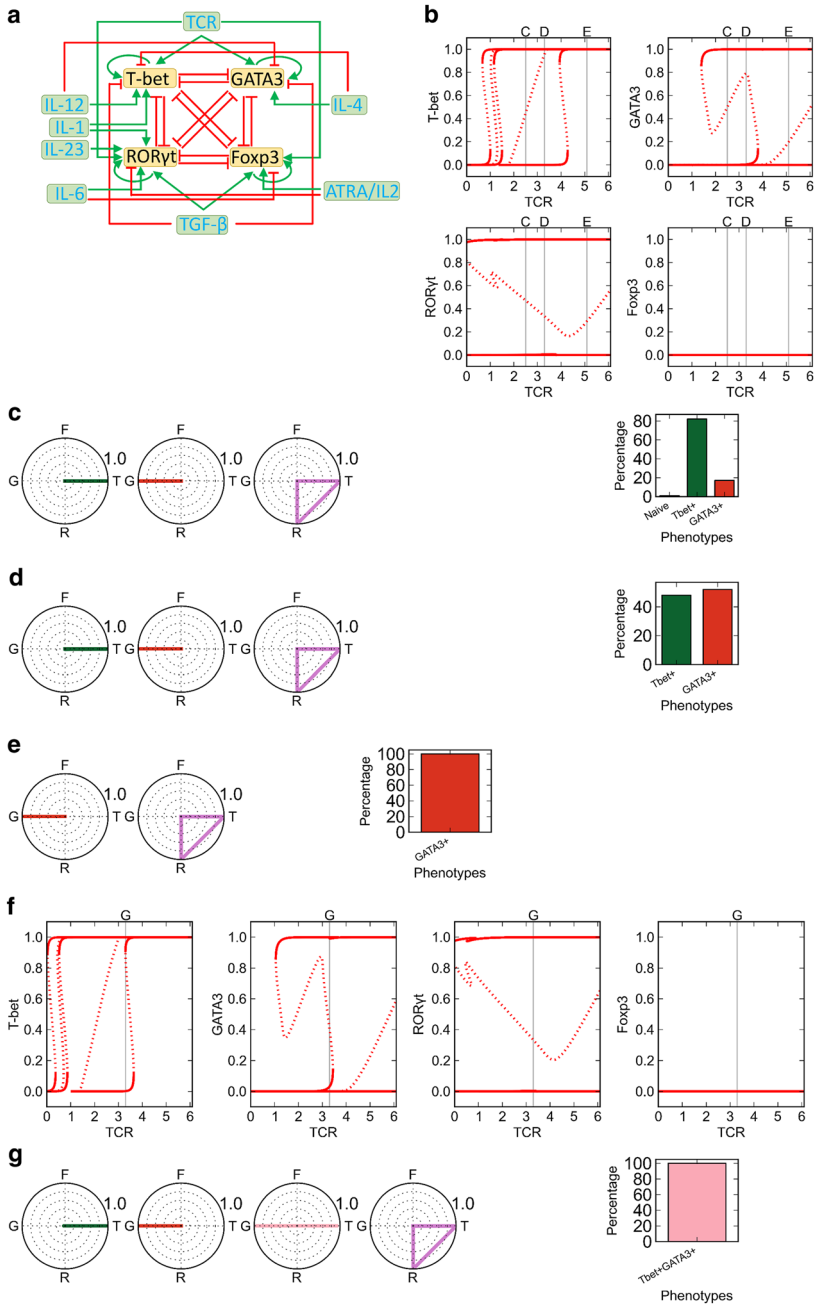


Fig. 4 Analysis of the CD4⁺ T cell model. **a** Influence diagram of the model. **b** Bifurcation diagrams with respect to TCR. *Solid curves, dashed curves and vertical gray lines* as in Fig. 1. **c–e** Radar plots and bar charts as in Fig. 1. **f** Bifurcation diagrams with respect to TCR in the presence of 25 units of IL-12 and 25 units of IL-4. **g** Radar plots (as in Fig. 1) and simulation results with TCR signal indicated in (f) (Color figure online)

differentiation of T-bet-GATA3 double-positive phenotype (Fig. 4f, g), consistent with the observations by Fang et al. (2013), Peine et al. (2013).

Heterogeneous differentiation of T_H1 and T_H17 cells can be reproduced by the model as well. As shown in Fig. 5a, b, in the presence of 5 units of IL-23, 5 units of IL-6 and 5 units of IL-1, four stable steady states (T-bet-positive, GATA3-positive, Foxp3-positive, and T-bet-ROR γ t double-positive) coexist for TCR = 2.5 units. The simulation results (Fig. 5b, bar chart) show that a population of cells differentiates primarily into T-bet-ROR γ t double-positive cells (20 %) and T-bet-positive cells (80 %), which is consistent with the observation by Ghoreschi et al. (2010).

The model reproduced heterogeneous differentiation of T_H17 (ROR γ t-positive) and iT_{Reg} (Foxp3-positive) cells under the condition of 5 units of TGF- β , 2.5 units of TCR signal, 0.25 units of anti-IFN γ and 0.75 units of anti-IL4 (Fig. 5c, d). A significant fraction of ROR γ t-Foxp3 double-positive cells are also obtained under these conditions, as observed by Zhou et al. (2008). The model predicts that the double-positive phenotype is stable only with sufficient amount (> 4 units) of exogenous TGF- β and that the single-positive cells can be stable without the exogenous TGF- β after the completion of differentiation.

A list of simulation results and corresponding experimental evidences is provided in Table 1.

3 Discussion

Early mathematical models of CD4⁺ T cells mainly focused on robustness of their differentiation process (Hofer et al. 2002; Mendoza 2006; van den Ham and de Boer 2008; Yates et al. 2004). Our recent models took into account heterogeneous differentiation involving two master regulators (Hong et al. 2011, 2012). Similar modeling studies have been done for other biological systems (Bell et al. 2007; Chang et al. 2008; Guantes and Poyatos 2008; Huang et al. 2007). However, all of these models limited their scope to two mutually inhibiting factors. Cinquin and Demongeot have identified a number of differentiation systems for which a generic motif with four mutually inhibiting transcription factors could be a reasonable model (Cinquin and Demongeot 2002, 2005). A similar network has been analyzed for segment determination process in *Drosophila* (Manu et al. 2009). The framework presented here provides a novel analytic tool for understanding multi-stability in dynamical systems with many mutual-inhibition motifs, to extend the theoretical results of Cinquin and Demongeot, and others (Cinquin and Demongeot 2002, 2005; Manu et al. 2009; Mendoza 2013; Naldi et al. 2010).

Although the models presented in this study have three or four master regulators, the framework can be easily extended to more than four master regulators, which will be necessary as more lineages and master regulators are being discovered in CD4⁺ T cells. For example, the recently discovered follicular T cells (T_{FH}) (Crotty 2011), together with their master regulator BCL-6, are known to participate in mutual-inhibition relationships (Kusam et al. 2003). When more information on this lineage becomes available, it can be included in the model, and the approach presented here can be used to study heterogeneous differentiation involving five master regulators. In addition, using

Table 1 Experimental results used to constrain the model of CD4⁺ T cells

Constraint	Experimental conditions of differentiation induction	Model conditions for exogenous signals	Cell population observed experimentally	Quantitative constraints summarized from experiments	Evidence
2	Exogenous polarizing signals alone	TGF-β: 8; anti-IL-4: 0.75; anti-IFNγ: 0.25	No induction of differentiation	Naïve > 85 %	Yamashita et al. (1999), Zhou et al. (2008)
5		TGF-β: 8; anti-IL-4: 0.75; anti-IFNγ: 0.25; IL-6: 5			
7		TGF-β: 8; anti-IL-4: 0.75; anti-IFNγ: 0.25; ATRA: 0.5			
10		IL-23: 5; IL-6: 6; IL-1: 5			
11		IL-12: 5			
13		IL-4: 5			
12	Low dose of antigenic stimulant (TCR signal) and IL-12	TCR:2.5; IL-12:5	Homogeneous differentiation of T _H 1	T-bet ⁺ > 50 %, GATA3 ⁺ < 5 %	Yamashita et al. (1999)
14	Low dose of antigenic stimulant (TCR signal) and IL-4	TCR: 2.5; IL-4: 5	Homogeneous differentiation of T _H 2	GATA3 ⁺ > 50 %, T-bet ⁺ < 5 %	Yamashita et al. (1999)
22	Antigenic stimulant in the presence of IL-4	TCR: 2.5; IL-4: 0.3	Heterogeneous differentiation of T _H 1 and T _H 2	T-bet ⁺ > 10 %, GATA3 ⁺ > 10 %	Messi et al. (2003), Yamashita et al. (1999)
15	Increasing strengths of TCR signal	TCR: 2.5	A spectrum of heterogeneous populations with increasing percentages of T _H 2 cells and decreasing percentage of T _H 1 cells	70 % < T-bet ⁺ < 90, 10 % < GATA3 ⁺ < 30 %	Hosken et al. (1995), Yamashita et al. (1999)
16		TCR: 3		50 % < T-bet ⁺ < 70, 30 % < GATA3 ⁺ < 50 %	

Table 1 continued

Constraint	Experimental conditions of differentiation induction	Model conditions for exogenous signals	Cell population observed experimentally	Quantitative constraints summarized from experiments	Evidence
17		TCR: 3.3		30% < T-bet ⁺ < 50, 50% < GATA3 ⁺ < 70 %	
18		TCR: 5.1		T-bet ⁺ < 15 %, GATA3 ⁺ > 85 %	
19	Blocking GATA3-IL4 feedback by antibodies against IL-4 and inducing with TCR signal	TCR: 2.5; anti-IL4: 0.75	No TH2 cells are observed	GATA3 ⁺ < 5 %	Maruyama et al. (2011)
9	TCR signal, IL-6 signal and IL-23+IL-1 signal	TCR: 2.5; IL-6:5; IL-1: 5	Heterogeneous differentiation of T-bet ⁺ RORγt ⁻ cells and T-bet ⁺ RORγt ⁺ cells.	40% < T-bet ⁺ < 80 %, 20% < T-bet ⁺ RORγt ⁺ < 60 %	Ghoreschi et al. (2010)
1	TCR signal and TGF-β signal	TCR: 2.5; TGF-β: 8; anti-IL-4: 0.75; anti-IFNγ: 0.25	Heterogeneous differentiation of RORγt ⁺ , Foxp3 ⁺ and RORγt ⁺ Foxp3 ⁺ cells	RORγt ⁺ > 15 %, Foxp3 ⁺ > 15 %, RORγt ⁺ Foxp3 ⁺ > 15 %	Zhou et al. (2008)
4	TCR signal and TGF-β+IL-6 signal	TCR: 2.5; TGF-β: 8; anti-IL-4: 0.75; anti-IFNγ: 0.25; IL-6: 5	The cell population is dominated by T-bet ⁻ RORγt ⁺ cells	RORγt ⁺ > 40 %, Foxp3 ⁺ + RORγt ⁺ Foxp3 ⁺ < 15 %, T-bet ⁺ < 5 %, T-bet ⁺ RORγt ⁺ < 5 %	Ghoreschi et al. (2010)
8	Knocking out T-bet genes and inducing with TCR signal in combined with IL-23+IL-1 signal	ω _{T-bet} ⁰ : -10; TCR: 2.5; IL-23: 5; IL-6: 5; IL-1: 5	Homogeneous differentiation of T-bet ⁻ RORγt ⁺ cells	RORγt ⁺ > 30 %, T-bet ⁺ RORγt ⁺ < 5 %	Ghoreschi et al. (2010)
21	Knocking out T-bet genes and inducing with TCR signal in combined with TGF-β signal	ω _{T-bet} ⁰ : -10; TCR: 2.5; TGF-β: 8	Homogeneous differentiation of T-bet ⁻ RORγt ⁺ cells	RORγt ⁺ > 20 %, T-bet ⁺ RORγt ⁺ < 5 %	Ghoreschi et al. (2010)

Table 1 continued

Constraint	Experimental conditions of differentiation induction	Model conditions for exogenous signals	Cell population observed experimentally	Quantitative constraints summarized from experiments	Evidence
20	Knocking out T-bet genes and inducing with TCR signal	ω_{T-bet}^0 : -10; TCR: 2.5	Homogeneous differentiation of GATA3 ⁺ cells	GATA3 ⁺ > 20 %, T-bet ⁺ < 5 %	Ghoreschi et al. (2010)
3	TGF- β +TCR signal and weak IL-6 signal	TCR: 2.5; TGF- β : 8; anti-IL-4: 0.75; anti-IFN γ : 0.25; IL-6: 1.5	Heterogeneous differentiation of ROR γ t ⁺ and Foxp3 ⁺ cells	25 % < ROR γ t ⁺ < 45 %, Foxp3 ⁺ + ROR γ t ⁺ Foxp3 ⁺ > 20 %	Zhou et al. (2008)
6	TGF- β +TCR signal and ATRA signal	TCR: 2.5; TGF- β : 8; anti-IL-4: 0.75; anti-IFN γ : 0.25; ATRA: 0.5	The cell population is dominated by the Foxp3 ⁺ cells	ROR γ t ⁺ < 5 %, Foxp3 ⁺ +ROR γ t ⁺ Foxp3 ⁺ > 40 %	Mucida et al. (2007)
Not used for constraint	TCR, IL-12 and IL-4 signals	TCR: 3.3; IL-12: 25; IL-4: 25	Homogeneous differentiation of T-bet ⁺ GATA3 ⁺ cells	T-bet ⁺ GATA3 ⁺ > 95 %	Fang et al. (2013), Peine et al. (2013)

Constraints 2, 5, 7, 10, 11, 13 all belong to the same experimental conditions (exogenous polarizing signals alone) and in all cases there is no induction of differentiation. Constraints 15–18 are grouped together under a common experimental condition (increasing strength of TCR signal) and they show an increasing/decreasing percentage of TH2/TH1 cells, respectively

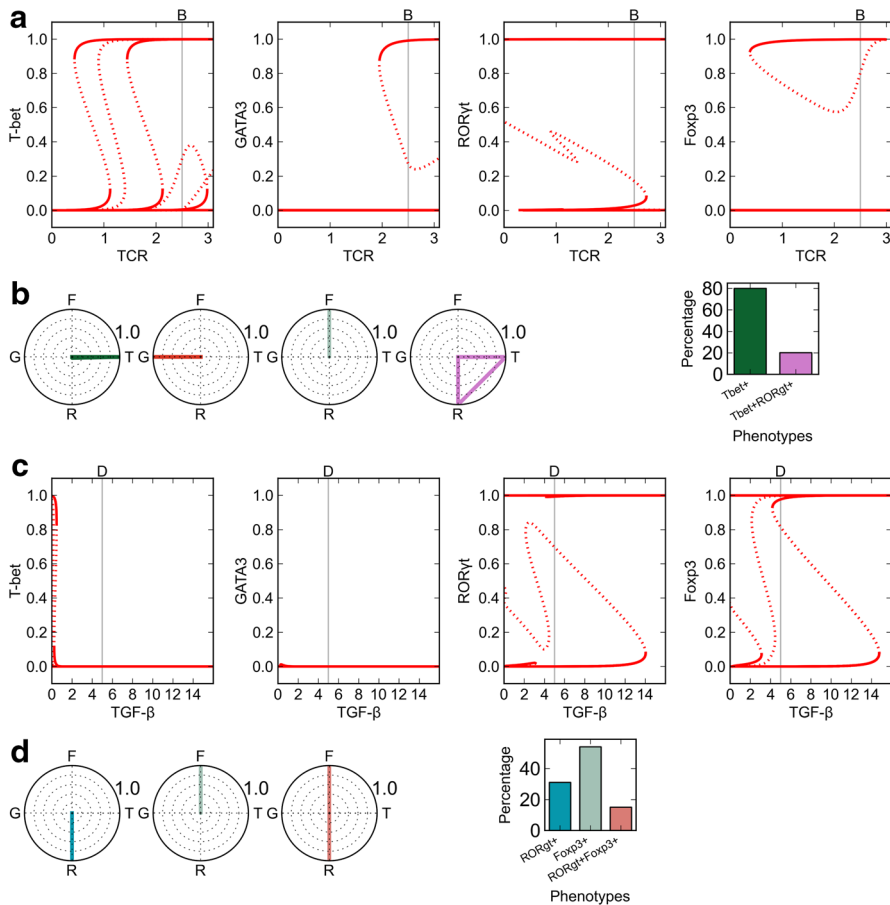


Fig. 5 Analysis of the $CD4^+$ T cell model under additional conditions. **a** Bifurcation diagrams with respect to TCR in the presence of 5 units of IL-23, 5 units of IL-6 and 5 units of IL-1. Solid curves, dashed curves and vertical gray lines as in Fig. 1. **b** Radar plots and bar charts as in Fig. 1. **c** Bifurcation diagrams with respect to TGF- β in the presence of 2.5 units of TCR, 0.25 units of anti-IFN γ and 0.75 units of anti-IL4 (Color figure online)

a mathematical model for two master regulators, Huang et al. (2007) demonstrated that near-symmetrical bifurcation can be critical for heterogeneous differentiation of two lineages of blood cells, suggesting that heterogeneous differentiation might be a common phenomenon in biological systems. Potentially, our framework for understanding heterogeneous differentiation involving more than two lineages in the neighborhood of highly symmetrical bifurcation points can be applied to biological systems other than $CD4^+$ T cells.

We illustrated the general bifurcation scenario for perfectly symmetrical systems as well as systems with slightly asymmetrical parameter values. For the general case, far from symmetrical bifurcation points, the bifurcation scenario is much more complex and difficult to study systematically. The major difference between a perfectly symmetrical case and an asymmetrical case is that in the symmetrical case, a particular

value of signal strength $S1$ can only produce cells with a definite number of over-expressed master regulators, e.g., in Fig 3, single-positive cells and double-positive cells are found in distinct regions of $S1$ parameter values. For asymmetrical cases, however, cells with different numbers of over-expressed master regulators can coexist for the same $S1$ value (e.g., Fig. 4c). Nonetheless, analysis of systems with perfect or nearly perfect symmetry is useful for understanding asymmetrical systems. From the symmetrical case, we understand which types of steady states can possibly be generated by the gene network and how they arise, and any of these states might be found in an asymmetrical system. In addition, although the asymmetrical bifurcation can be very different from the perfectly symmetrical bifurcation, some general phenomenon are conserved. For example, under conditions of low external signal strength (i.e., low TCR or cytokine-free conditions), the single-positive phenotype is easier to be stabilized than the double-positive state (see, e.g., Fig 4c–f).

Our analysis shows that a double-positive phenotype is a stable cellular state rather than a transient progenitor during differentiation. The existence of double-positive states is due to the external signal overriding the internal mutual inhibitory relationships. This explanation is consistent with the observations that external cytokine signals can give rise to T-bet-GATA3 double-positive cells and that blocking such signals resulted in a heterogeneous mixture of T-bet⁺ and GATA3⁺ single-positive cells (Fang et al. 2013) [also see the commentary article by Huang (2013)]. Peine et al. (Peine et al. 2013) also demonstrated that similar signaling conditions can produce T-bet-GATA3 double-positive cells. In addition, this phenotype can arise naturally without persistent antigenic stimulus (Peine et al. 2013). In our model, however, this double-positive phenotype requires the presence of TCR signaling. This fault of the model may be due to its lack of positive feedback loops on longer time scales (discussed below).

Experimental studies of CD4⁺ T cells had focused on ‘polarizing’ conditions, for which one phenotype dominates a population of differentiating cells. These studies provide useful information on signaling pathways controlling specific lineages of CD4⁺ T cells, but they have limited relevance to physiological conditions, for which differentiation often involves multiple phenotypes. Recently, heterogeneous differentiation of T_H1 and T_H2 cells with mixtures of opposing polarizing cytokines was studied quantitatively by Antebi et al. (2013). Due to the large variety of CD4⁺ T cells, more experimental studies on heterogeneous population of these cells are needed, and our theoretical framework can provide a basis for understanding the system and designing experiments.

Our model assumes mutual inhibitory relationships among all master regulators. Although experimental demonstration of direct inhibition is still lacking for some of the assumed interactions (Zhu and Paul 2010), indirect evidences support our assumptions. For example, T-bet may not inhibit GATA3 directly (Hwang et al. 2005), but retroviral T-bet expression in developing and established T_H2 cells leads to down-regulation of GATA3 levels (Usui et al. 2006), and GATA3 target genes are also inhibited by T-bet (Hwang et al. 2005; Szabo et al. 2000). Moreover, mutually exclusive expression of T-bet and GATA3 is observed in some experimental conditions (Fang et al. 2013). Therefore, it is reasonable to assume a mutual-inhibition relationship between these two master regulators. Nevertheless, our assumptions on direct mutual inhibitions need to be validated experimentally in the future.

Our model focuses on heterogeneous differentiation that occurs in the initial stages of the CD4⁺ T cell lineage specification. Signaling events on a longer time scale (i.e., more than a week) may have significant influences on the derived populations, and these factors might not be captured by our modeling framework. In particular, these events might be responsible for the irreversible commitment of differentiated cell lines (Murphy et al. 1996). Irreversible differentiation of T cell phenotypes are not observed in our simulations (e.g., Fig. 4c). Nonetheless, our model can potentially be extended to take into account irreversible differentiation by adding some slow positive feedback loops that reinforce the differentiation on a longer time scale. These positive feedback loops might be additional autocrine effects or epigenetic modifications. In addition, our model for CD4⁺ T cells neglects the fact that T cell differentiation can be influenced by inter-cellular signals. In other words, cytokines secreted by one cell can influence the behaviors of other cells. A consideration of such cross talk will be the subject of future studies. In addition, the rates of proliferation of different cell types can have significant effects on the composition of the heterogeneous cell population, as observed in CD8⁺ T cells (Gerlach et al. 2013). Therefore, a consideration of cell proliferation is needed in future models.

Acknowledgments This work was supported by Grant R01GM078989-07 from the National Institutes of Health to JJT. The authors thank the two anonymous reviewers for their insightful and constructive comments, which helped us to improve the manuscript

Appendix: Methods

Dynamical Models

We build mathematical models of three different signaling motifs (two generic motifs and one motif specific to T cell differentiation). For each case, we use a generic form of ordinary differential equations (ODEs) suitable for describing both gene expression and protein interaction networks (Mjolsness et al. 1991; Tyson and Novak 2010; Wilson and Cowan 1972). Each ODE in the model has the form:

$$\begin{aligned} \frac{dX_i}{dt} &= \gamma_i (F(\sigma_i W_i) - X_i) \\ F(\sigma W) &= 1 / \left(1 + e^{-\sigma W} \right) \\ W_i &= \left(\omega_i^o + \sum_j^N \omega_{j \rightarrow i} X_j \right) \\ i &= 1, \dots, N \end{aligned} \quad (1)$$

Here, X_i is the activity or concentration of protein i . On a time scale $= 1/\gamma_i$, $X_i(t)$ relaxes toward a value determined by the sigmoidal function, F , which has a steepness set by σ_i . The basal value of F , in the absence of any influencing factors, is determined by ω_i^o . The coefficients $\omega_{j \rightarrow i}$ determine the influence of protein j on protein i . N is the total number of proteins in the network.

All variables and parameters are dimensionless. One time unit in the simulations corresponds to approximately 1 day. Basal parameter values of each model are listed in supplementary tables (see ‘Cell-to-Cell Variability’ subsection for details).

All simulations and bifurcation analyses were performed with PyDSTool, a software environment for dynamical systems (Clewley 2012).

Bifurcation Diagrams and Steady State Radar Plots

One parameter bifurcation diagrams were plotted by following the steady state solution of the ODEs with change in the value of a control parameter.

In order to analyze the behavior of multi-variable systems, we use radar plots to illustrate the steady states for a particular parameter set. A radar plot depicts the expression level of each key state variable (i.e., master regulator) on one sub-plot, and multiple sub-plots describe multiple steady states. In principle, a radar plot can illustrate unstable steady states as well as stable steady states, but we plot only stable steady states, which correspond to observable cell phenotypes.

Cell-to-Cell Variability

To account for cell-to-cell variability in a population, we made many simulations of the system of ODEs, each time with a slightly different choice of parameter values (to represent slight differences from cell to cell). We assumed that the value of each parameter conforms to a normal distribution with $CV = 0.05$ ($CV = \text{coefficient of variation} = \text{standard deviation}/\text{mean}$). We refer to the mean value for each parameter distribution as the ‘basal’ value of that parameter. In the bifurcation analysis of the dynamical system, we consider an imaginary cell that adopts the basal value for each of its parameters, and we define this cell as the ‘average’ cell. However, none of the cells in the simulated population is likely to be this average cell, because every parameter value is likely to deviate a little from the basal value.

Simulation Procedure

In order to simulate the induced differentiation process, we first solved the ODEs numerically with small initial values of master regulator concentrations in the absence of any exogenous signals. After a short period of time, each simulated cell found its own, stable ‘naïve’ steady state in which all master regulators are expressed at low level. Next, we changed the exogenous signals to the values listed in Supplementary Tables S1, S2 and S3 and continued the numerical simulation. Each cell arrived at its corresponding ‘induced’ phenotype, which might vary from cell to cell because of the parametric variability of the population. The expression level of each protein in the network ranges from 0 to 1 unit, and we made the simple assumption that a protein is ‘expressed’ if its level is greater than 0.5 units. We defined the derived population as ‘heterogeneous’ if it contained cells with more than one phenotype.

Parameter Optimization

Before starting to optimize the model parameters, we defined a hyperbox in the parameter space that is bounded by biologically plausible parameter ranges. These ranges are listed in Supplementary Table S3. A population of 200 parameter vectors, generated by Latin hypercube sampling (LHS), captured from 3 to 14 of the 22 experimental constraints that are listed in Table 1 (there are 22 independent constraints in 14 different experimental conditions). Starting with this population, we next implemented Differential Evolution (DE). The two-stage optimization approach based on LHS and DE has been presented previously by [Oguz et al. \(2013\)](#). Details of LHS and DE are provided in the Supplementary Text. For the initial round of DE, we used an aggressive mutation operator ($F = 0.1$ in Eq. (2) of Supplementary Text) and a non-greedy selection condition. After 900 generations of DE, we obtained several parameter vectors that captured 19 of the 21 experimental constraints. We also identified that Constraint 1 (shown in Table 1) was the experimental constraint with the lowest acceptance (0.03 %) among the parameter vectors generated by DE ($200 \times 900 = 180,000$ vectors). In the second round of DE, starting with the 57 parameter vectors that captured Constraint 1, we used a more conservative mutation operator ($F = 0.01$) and a non-greedy selection condition in order to maximize the number of total constraints captured. In addition, we enforced Constraint 1 at every step; a mutant vector could only replace a parent if it captured Constraint 1. After ~ 500 generations, we found several feasible parameter vectors that captured 18–22 of the 22 experimental constraints. The optimized parameter values from the most robust feasible vector are given in Supplementary Table S3. The robustness measure that we used in the robustness analysis is described in Sect. 3 of the Supplementary Text (last paragraph).

References

- Antebi YE et al (2013) Mapping differentiation under mixed culture conditions reveals a tunable continuum of T cell fates. *PLoS Biol* 11:e1001616. doi:[10.1371/journal.pbio.1001616](https://doi.org/10.1371/journal.pbio.1001616)
- Ball J, Schaeffer D (1983) Bifurcation and stability of homogeneous equilibrium configurations of an elastic body under dead-load tractions. In: *Mathematical proceedings of the Cambridge philosophical society*. Cambridge Univ Press, Cambridge, pp 315–339
- Bell ML, Earl JB, Britt SG (2007) Two types of Drosophila R7 photoreceptor cells are arranged randomly: a model for stochastic cell-fate determination. *J Comp Neurol* 502:75–85. doi:[10.1002/cne.21298](https://doi.org/10.1002/cne.21298)
- Chang HH, Hemberg M, Barahona M, Ingber DE, Huang S (2008) Transcriptome-wide noise controls lineage choice in mammalian progenitor cells. *Nature* 453:544–547. doi:[10.1038/nature06965](https://doi.org/10.1038/nature06965)
- Cinquin O, Demongeot J (2002) Positive and negative feedback: striking a balance between necessary antagonists. *J Theor Biol* 216:229–241. doi:[10.1006/jtbi.2002.2544](https://doi.org/10.1006/jtbi.2002.2544)
- Cinquin O, Demongeot J (2005) High-dimensional switches and the modelling of cellular differentiation. *J Theor Biol* 233:391–411. doi:[10.1016/j.jtbi.2004.10.027](https://doi.org/10.1016/j.jtbi.2004.10.027)
- Clewley R (2012) Hybrid models and biological model reduction with PyDSTool. *PLoS Comput Biol* 8:e1002628. doi:[10.1371/journal.pcbi.1002628](https://doi.org/10.1371/journal.pcbi.1002628)
- Crotty S (2011) Follicular helper CD4 T cells (TFH). *Annu Rev Immunol* 29:621–663. doi:[10.1146/annurev-immunol-031210-101400](https://doi.org/10.1146/annurev-immunol-031210-101400)
- Fang M, Xie H, Dougan SK, Ploegh H, van Oudenaarden A (2013) Stochastic cytokine expression induces mixed T helper cell states. *PLoS Biol* 11:e1001618–e1001618. doi:[10.1371/journal.pbio.1001618](https://doi.org/10.1371/journal.pbio.1001618)
- Fontenot JD, Gavin MA, Rudensky AY (2003) Foxp3 programs the development and function of CD4+CD25+ regulatory T cells. *Nat Immunol* 4:330–336. doi:[10.1038/ni904](https://doi.org/10.1038/ni904)

- Gerlach C et al (2013) Heterogeneous differentiation patterns of individual CD8+ T cells. *Science* 340:635–639. doi:[10.1126/science.1235487](https://doi.org/10.1126/science.1235487)
- Ghoreschi K et al (2010) Generation of pathogenic T(H)17 cells in the absence of TGF-beta signalling. *Nature* 467:967–971. doi:[10.1038/nature09447](https://doi.org/10.1038/nature09447)
- Golubitsky M, Stewart I, Schaeffer DG (1988) Singularities and groups in bifurcation theory, vol. II. Applied Mathematical Sciences
- Guantes R, Poyatos JF (2008) Multistable decision switches for flexible control of epigenetic differentiation. *PLoS Comput Biol* 4:e1000235. doi:[10.1371/journal.pcbi.1000235](https://doi.org/10.1371/journal.pcbi.1000235)
- Hofer T, Nathansen H, Lohning M, Radbruch A, Heinrich R (2002) GATA-3 transcriptional imprinting in Th2 lymphocytes: a mathematical model. *Proc Natl Acad Sci USA* 99:9364–9368. doi:[10.1073/pnas.142284699](https://doi.org/10.1073/pnas.142284699)
- Hong T, Xing J, Li L, Tyson JJ (2011) A mathematical model for the reciprocal differentiation of T helper 17 cells and induced regulatory T cells. *PLoS Comput Biol* 7:e1002122. doi:[10.1371/journal.pcbi.1002122](https://doi.org/10.1371/journal.pcbi.1002122)
- Hong T, Xing J, Li L, Tyson JJ (2012) A simple theoretical framework for understanding heterogeneous differentiation of CD4+ T cells. *BMC Syst Biol* 6:66. doi:[10.1186/1752-0509-6-66](https://doi.org/10.1186/1752-0509-6-66)
- Hosken NA, Shibuya K, Heath AW, Murphy KM, O'Garra A (1995) The effect of antigen dose on CD4+ T helper cell phenotype development in a T cell receptor-alpha beta-transgenic model. *J Exp Med* 182:1579–1584
- Hsieh CS, Macatonia SE, Tripp CS, Wolf SF, O'Garra A, Murphy KM (1993) Development of TH1 CD4+ T cells through IL-12 produced by *Listeria*-induced macrophages. *Science* 260:547–549
- Huang S (2013) Hybrid T-helper cells: stabilizing the moderate center in a polarized system. *PLoS Biol* 11:e1001632–e1001632. doi:[10.1371/journal.pbio.1001632](https://doi.org/10.1371/journal.pbio.1001632)
- Huang S, Guo YP, May G, Enver T (2007) Bifurcation dynamics in lineage-commitment in bipotent progenitor cells. *Dev Biol* 305:695–713. doi:[10.1016/j.ydbio.2007.02.036](https://doi.org/10.1016/j.ydbio.2007.02.036)
- Hwang ES, Szabo SJ, Schwartzberg PL, Glimcher LH (2005) T helper cell fate specified by kinase-mediated interaction of T-bet with GATA-3. *Science* 307:430–433. doi:[10.1126/science.1103336](https://doi.org/10.1126/science.1103336)
- Ivanov II et al (2006) The orphan nuclear receptor RORgammat directs the differentiation program of proinflammatory IL-17+ T helper cells. *Cell* 126:1121–1133. doi:[10.1016/j.cell.2006.07.035](https://doi.org/10.1016/j.cell.2006.07.035)
- Kusam S, Toney LM, Sato H, Dent AL (2003) Inhibition of Th2 differentiation and GATA-3 expression by BCL-6. *J Immunol* 170:2435–2441
- Luckheeram RV, Zhou R, Verma AD, Xia B (2012) CD4(+)T cells: differentiation and functions. *Clin Dev Immunol* 2012:925135. doi:[10.1155/2012/925135](https://doi.org/10.1155/2012/925135)
- Manu SS et al (2009) Canalization of gene expression and domain shifts in the *Drosophila* blastoderm by dynamical attractors. *PLoS Comput Biol* 5:e1000303. doi:[10.1371/journal.pcbi.1000303](https://doi.org/10.1371/journal.pcbi.1000303)
- Maruyama T et al (2011) Control of the differentiation of regulatory T cells and T(H)17 cells by the DNA-binding inhibitor Id3. *Nat Immunol* 12:86–95. doi:[10.1038/ni.1965](https://doi.org/10.1038/ni.1965)
- Mendoza L (2006) A network model for the control of the differentiation process in Th cells. *Bio Syst* 84:101–114. doi:[10.1016/j.biosystems.2005.10.004](https://doi.org/10.1016/j.biosystems.2005.10.004)
- Mendoza L (2013) A virtual culture of CD4+ T lymphocytes. *Bull Math Biol*. doi:[10.1007/s11538-013-9814-9](https://doi.org/10.1007/s11538-013-9814-9)
- Messi M, Giacchetto I, Nagata K, Lanzavecchia A, Natoli G, Sallusto F (2003) Memory and flexibility of cytokine gene expression as separable properties of human T(H)1 and T(H)2 lymphocytes. *Nat Immunol* 4:78–86. doi:[10.1038/ni872](https://doi.org/10.1038/ni872)
- Mjolsness E, Sharp DH, Reintz J (1991) A connectionist model of development. *J Theor Biol* 152:429–453
- Mucida D, Park Y, Kim G, Turovskaya O, Scott I, Kronenberg M, Cheroute H (2007) Reciprocal TH17 and regulatory T cell differentiation mediated by retinoic acid. *Science* 317:256–260
- Murphy E, Shibuya K, Hosken N (1996) Reversibility of T helper 1 and 2 populations is lost after long-term stimulation. *J Exp Med* 183:901–913
- Murphy KM, Stockinger B (2010) Effector T cell plasticity: flexibility in the face of changing circumstances. *Nat Immunol* 11:674–680. doi:[10.1038/ni.1899](https://doi.org/10.1038/ni.1899)
- Naldi A, Carneiro J, Chaouiya C, Thieffry D (2010) Diversity and plasticity of Th cell types predicted from regulatory network modelling. *PLoS Comput Biol* 6:e1000912. doi:[10.1371/journal.pcbi.1000912](https://doi.org/10.1371/journal.pcbi.1000912)
- O'Shea JJ, Paul WE (2010) Mechanisms underlying lineage commitment and plasticity of helper CD4+ T cells. *Science* 327:1098–1102. doi:[10.1126/science.1178334](https://doi.org/10.1126/science.1178334)

- Oguz C, Laomettachit T, Chen KC, Watson LT, Baumann WT, Tyson JJ (2013) Optimization and model reduction in the high dimensional parameter space of a budding yeast cell cycle model. *BMC Syst Biol* 7:53. doi:[10.1186/1752-0509-7-53](https://doi.org/10.1186/1752-0509-7-53)
- Peine M et al (2013) Stable T-bet(+)GATA-3(+) Th1/Th2 hybrid cells arise in vivo, can develop directly from naive precursors, and limit immunopathologic inflammation. *PLoS Biol* 11:e1001633–e1001633. doi:[10.1371/journal.pbio.1001633](https://doi.org/10.1371/journal.pbio.1001633)
- Szabo SJ, Kim ST, Costa GL, Zhang X, Fathman CG, Glimcher LH (2000) A novel transcription factor, T-bet, directs Th1 lineage commitment. *Cell* 100:655–669
- Tyson JJ, Novak B (2010) Functional motifs in biochemical reaction networks. *Annu Rev Phys Chem* 61:219–240. doi:[10.1146/annurev.physchem.012809.103457](https://doi.org/10.1146/annurev.physchem.012809.103457)
- Usui T, Preiss JC, Kanno Y, Yao ZJ, Bream JH, O’Shea JJ, Strober W (2006) T-bet regulates Th1 responses through essential effects on GATA-3 function rather than on IFNG gene acetylation and transcription. *J Exp Med* 203:755–766. doi:[10.1084/jem.20052165](https://doi.org/10.1084/jem.20052165)
- van den Ham HJ, de Boer RJ (2008) From the two-dimensional Th1 and Th2 phenotypes to high-dimensional models for gene regulation. *Int Immunol* 20:1269–1277. doi:[10.1093/intimm/dxn093](https://doi.org/10.1093/intimm/dxn093)
- Wilson HR, Cowan JD (1972) Excitatory and inhibitory interactions in localized populations of model neurons. *Biophys J* 12:1–24. doi:[10.1016/S0006-3495\(72\)86068-5](https://doi.org/10.1016/S0006-3495(72)86068-5)
- Yamashita M, Kimura M, Kubo M, Shimizu C, Tada T, Perlmutter RM, Nakayama T (1999) T cell antigen receptor-mediated activation of the Ras/mitogen-activated protein kinase pathway controls interleukin 4 receptor function and type-2 helper T cell differentiation. *Proc Natl Acad Sci USA* 96:1024–1029
- Yates A, Callard R, Stark J (2004) Combining cytokine signalling with T-bet and GATA-3 regulation in Th1 and Th2 differentiation: a model for cellular decision-making. *J Theor Biol* 231:181–196. doi:[10.1016/j.jtbi.2004.06.013](https://doi.org/10.1016/j.jtbi.2004.06.013)
- Zheng W, Flavell RA (1997) The transcription factor GATA-3 is necessary and sufficient for Th2 cytokine gene expression in CD4 T cells. *Cell* 89:587–596
- Zhou L et al (2008) TGF-beta-induced Foxp3 inhibits T(H)17 cell differentiation by antagonizing RORgamma function. *Nature* 453:236–240. doi:[10.1038/nature06878](https://doi.org/10.1038/nature06878)
- Zhu J, Paul WE (2010) Peripheral CD4(+) T-cell differentiation regulated by networks of cytokines and transcription factors. *Immunol Rev* 238:247–262. doi:[10.1111/j.1600-065X.2010.00951.x](https://doi.org/10.1111/j.1600-065X.2010.00951.x)
- Zhu J, Yamane H, Paul WE (2010) Differentiation of effector CD4 T cell populations. *Annu Rev Immunol* 28:445–489. doi:[10.1146/annurev-immunol-030409-101212](https://doi.org/10.1146/annurev-immunol-030409-101212)